



# Electrochemical determination of *Saccharomyces cerevisiae* sp using glassy carbon electrodes modified with oxidized multi-walled carbon nanotubes dispersed in water –Nafion®

Isabel Acevedo Restrepo<sup>a,\*</sup>, Lucas Blandón Naranjo<sup>a</sup>, Jorge Hoyos-Arbeláez<sup>b</sup>,  
Mario Víctor Vázquez<sup>a</sup>, Silvia Gutiérrez Granados<sup>c</sup>, Juliana Palacio<sup>d</sup>

<sup>a</sup> Interdisciplinary Group of Molecular Studies (GIEM), Chemistry Institute, Faculty of Exact and Natural Sciences, Universidad de Antioquia, Street 67 No. 53-108, Medellín, Colombia

<sup>b</sup> BIOALI Research Group, Food Department, Faculty of Pharmaceutical and Food Sciences, Universidad de Antioquia, Street 67 No. 53-108, Medellín, Colombia

<sup>c</sup> Department of Chemistry, Division of Exact and Natural Sciences, Campus Guanajuato, Universidad de Guanajuato, Cerro de la Venada s/n, Colonia Pueblito de Rocha, 36040, Guanajuato, Mexico

<sup>d</sup> Materials Science Research Group, Chemistry Institute, Faculty of Exact and Natural Sciences, Universidad de Antioquia, Street 70 No. 52-21, Medellín, Colombia

## ARTICLE INFO

### Keywords:

Yeast  
*Saccharomyces cerevisiae* sp  
Glassy carbon electrodes  
Nafion®  
Oxidized multi-walled carbon nanotubes  
Electrochemical determination

## ABSTRACT

The electrochemical behavior of *Saccharomyces cerevisiae* sp was studied using a glassy carbon electrode (GCE) modified with Nafion-dispersed oxidized multi-walled carbon nanotubes (OMWCNT). The morphology was studied using scanning electron microscopy (SEM), showing that the yeast sticks to the carbon nanotube surface instead of the glassy carbon surface. The redox couple  $\text{Fe}(\text{CN})_6^{4-}/\text{Fe}(\text{CN})_6^{3-}$  was used to determine the electroactive area and the heterogeneous transfer constant, which increased 80.5% and 108% respectively by the presence of nanotubes. The studies of the pH effect showed that the anodic potential decreases at alkaline pH and that the highest current intensity occurs at a pH value of 7.00. Studies of the scan rate effect have shown that yeast oxidation is an irreversible mixed control process in which two electrons participate. The relationship between yeast concentration and the anodic current density was studied using different electrochemical techniques obtaining the best analytical parameters through chronoamperometry. The linear range was between 3.36 and 6.52 g L<sup>-1</sup>, the limit of detection (LOD) and the limit of quantification (LOQ) were 0.98 g L<sup>-1</sup> and 3.36 g L<sup>-1</sup> respectively, and the sensibility obtained was 0.086 μA L g<sup>-1</sup> mm<sup>-2</sup>. These results show that the multi-walled carbon nanotubes in water and Nafion® allow obtaining an anodic signal corresponding to the yeast, which facilitates its quantification through electrochemical methodologies, favoring the reduction of analysis times and costs compared with other techniques.

## 1. Introduction

Yeast is a unicellular eukaryote belonging to the Fungi kingdom. Yeast reproduced by budding can be classified into Basidiomycetes (Filobasidiella, Rhodotorula) and Ascomycetes (Saccharomyces, Candida). They also have structural characteristics similar to the eukaryotes of plants and animals. There are more than 1500 species of yeast, 80% of which have biotechnological applications. *Saccharomyces cerevisiae* is a yeast best known precisely for its wide use in different bioprocesses. *Saccharomyces cerevisiae* belongs to the Ascomycetes family. It has an ellipsoid shape with an external diameter of 5–10 μm. This microorganism is attractive in biotechnology and the food industry

since it is not pathogenic, resists high concentrations of ethanol, butanol, and is the most studied eukaryotic cell, so it has served to understand the biology of this type of cell. *Saccharomyces cerevisiae* has many applications, much of them enhanced by the development of genetic and metabolic engineering (Hartwell, 1974; Legras et al., 2007; Shen et al., 2021; Turker, 2014; Zhong et al., 2021).

The new area in which the behavior of this yeast is a study object is electrochemistry. The electrochemical tools applied to the study of *S. cerevisiae* range from its use as a biological recognition element or as a test microorganism for evaluating the interaction of different materials with biological systems to the study of cellular inhibitors and the development of methodologies for its detection through electrochemical

\* Corresponding author.

E-mail address: [disabel.acevedo@udea.edu.co](mailto:disabel.acevedo@udea.edu.co) (I. Acevedo Restrepo).

<https://doi.org/10.1016/j.crfs.2022.01.022>

Received 8 September 2021; Received in revised form 24 January 2022; Accepted 28 January 2022

Available online 5 February 2022

2665-9271/© 2022 Published by Elsevier B.V. This is an open access article under the CC BY-NC-ND license (<http://creativecommons.org/licenses/by-nc-nd/4.0/>).

techniques (D. Wang et al., 2003). Likewise, several works have tried to understand the cell-electrode interaction.

One of the most extended uses of *S. cerevisiae* in electrochemistry is in the design of electrochemical biosensors. For example, Barliková et al. (1991) developed a biosensor with *S. cerevisiae* and glucose oxidase for detecting sucrose, the linear range reached  $13 \times 10^{-3} \text{ mol L}^{-1}$ . Filipović et al. (Filipović et al., 2002) developed a cyanide biosensor in fruit spirits using *S. cerevisiae*. The results were compared by ISE – potentiometry, finding an average recovery of  $97.8 \pm 6.8\%$ . Campanella et al. (Campanella et al., 1996) developed biosensors with immobilized yeast for toxicity studies of organic compounds or drugs in aqueous environmental matrices. Lehmann et al. (Lehmann et al., 2000) developed a biosensor with immobilized *S. cerevisiae* cells on a capillary to quantify  $\text{Cu}^{2+}$  ions in a range between 0.5 and 2 mM  $\text{CuSO}_4$ . Garjonyte et al. (Garjonyte et al., 2006) applied layers of yeast on a carbon paste electrode for developing a biosensor for lactic acid determination in milk and dairy products. The linear range was up to 1 mM. Akyilmaz et al. (Akyilmaz et al., 2007) used *S. cerevisiae* to design a biosensor for L-lysine determination. The linear range was between 1 and 10  $\mu\text{M}$ .

Other researchers link electrochemistry with yeast. Corton et al. (Corton et al., 2001) found a direct electrochemical methodology for identifying microbial species, between them, *S. cerevisiae*, using a gold working electrode and CV directly on cell culture samples without pretreatment. Zhao et al. (Zhao et al., 2008) used platinum microelectrodes for studying the inhibition of *S. cerevisiae* by acetic acid. Posseckardt et al. (Posseckardt et al., 2018) developed a methodology for the viability of cell quantification by electrochemical impedance microscopy using platinum screen-printing electrodes (SPE), finding an increment of the measurements in living cells. Valiūnienė et al. (Valiūnienė et al., 2020) developed a methodology for differentiating active and inactive cells of *S. cerevisiae* by electrochemical impedance microscopy. The charge transfer resistance of active cells was 1.5 times lower than inactivated yeast cells.

Regarding the electrochemical behavior of yeast, we can highlight the researches of Matsunaga et al. (T Matsunaga et al., 1979; Matsunaga and Namba, 1984). The electroactive character of *S. cerevisiae* was studied using a graphite electrode. The microorganism was irreversibly oxidized between 0.75 V–0.80 V (versus SCE Reference electrode). The authors suggested that oxidation involves two electrons and that the reaction is possible due to the coenzyme A bound to the internal part of the cell wall. Ci, YX et al. (Ci et al., 1997) used graphite electrodes and the cyclic voltammetry technique to show that the relationship between the peak current and the time of fermentation of yeast is similar to the cell growth curve. Han et al. (2000) studied the yeast behavior on glassy carbon electrodes (GCE) modified with tetracycline. The authors agreed with Matsunaga et al. that two electrons are involved in the oxidation reaction, but they attribute it to the cytochrome oxidase. Recently, Villalonga et al. (Villalonga et al., 2019) determined the total content of *Brettanomyces bruxellensis* and *S. cerevisiae* in wine, using graphite SPE modified with superparamagnetic  $\text{Fe}_3\text{O}_4 @ \text{SiO}_2$  core-shell nanoparticles.

Hubenova et al. (Rawson et al., 2012) had investigated the interaction electrode - cell. They determined that there is a direct exchange of electrons from the yeast to the electrode. The electrode cannot make direct contact with redox centers of the yeast then the authors have proposed that the electrochemical signal can be attributable to a soluble electroactive substance excreted from inside the cell or that is united to the external cell wall.

However, we do not know the interaction of the microorganism with carbonaceous nanomaterials, for example, carbon nanotubes, or if a direct response on electrodes modified with these materials is possible. We don't know if the scan rate or pH factors affect the yeast electrochemical response or the behavior of the microorganism with other electroanalytical techniques. In this sense, this work studies the electrochemical response of *S. cerevisiae* on OMWCNT and Nafion® as modifying agents of GCE without electrochemical mediators. We

developed a determination methodology to evaluate the possibility of using such sensors for *S. cerevisiae* determination.

## 2. Materials and methods

### 2.1. Materials, chemicals, and culture media

The commercial *Saccharomyces cerevisiae* sp yeast strain used in this study was from a local store. Yeast suspensions at different concentrations were prepared from a stock suspension of 50 g  $\text{L}^{-1}$ . All suspensions were prepared in a phosphate buffer solution (PBS) pH 7.00 and incubated at 37 °C for 15 min. Phosphate-buffered saline (PBS) concentration was 0.01 mol  $\text{L}^{-1}$  from monobasic sodium phosphate ( $\text{NaH}_2\text{PO}_4$ , Sigma) and dibasic sodium phosphate ( $\text{Na}_2\text{HPO}_4$ , Sigma); potassium chloride (KCl, Merck) 0.10 mol  $\text{L}^{-1}$  was used as a supporting electrolyte. For pH modifications, we used phosphoric acid ( $\text{H}_3\text{PO}_4$ ) 0.10 mol  $\text{L}^{-1}$  or sodium hydroxide (NaOH, Sigma) 0.10 mol  $\text{L}^{-1}$ . Potassium hexacyanoferrate (III) trihydrate solution ( $\text{K}_3[\text{Fe}(\text{CN})_6] \cdot 3\text{H}_2\text{O}$ , Sigma), at a concentration of  $1 \times 10^{-3}$  mol  $\text{L}^{-1}$  in KCl 0.10 mol  $\text{L}^{-1}$  was used to evaluate the electroactive area, heterogeneous transfer constant, and general behavior of the electrode.

The electrochemical experiments were performed in a three-electrode cell using an AUTOLAB PGSTAT 101 potentiostat (Utrecht, the Netherlands) with NOVA 1.11 software. The working electrode was a glassy carbon electrode (GCE), the reference electrode was an Ag/AgCl/KCl (3.0 M), and the auxiliary electrode was a platinum wire (all purchased in CH Instruments Inc, Texas, USA). Commercial multi-walled carbon nanotubes (MWCNTs, Nano-Lab, Waltham, Massachusetts, USA) were oxidized in a microwave-assisted acid medium for 15 min according to the method proposed by Blandón et al. (Blandón--Naranjo et al., 2018). Sodium hydroxide (NaOH, Sigma) 2.0 mol  $\text{L}^{-1}$  and Nafion® perfluorinated resin (Sigma-Aldrich, Missouri, USA) solution 5% weight in water were used as stabilizers and surface modifiers.

### 2.2. Glassy carbon electrode modification and characterization

1.5 mg of oxidized multi-walled carbon nanotubes were dispersed first in 50  $\mu\text{L}$  of NaOH 2.0 mol  $\text{L}^{-1}$ , followed by vortex agitation. Then, 50  $\mu\text{L}$  of Nafion was added and followed by vortex agitation. Finally, 900  $\mu\text{L}$  of distilled water was added with vortex agitation and ultrasonic bath for 30 min. The oxidized nanotubes stabilized with Nafion were named OMWCNT-N.

The electrodes were polished for 3 min with 1.0, 0.3, and 0.05  $\mu\text{m}$  alumina and rinsed with abundant distilled water before the measurements and modification of the GCE. Subsequently, the GCE was placed in ethanol and sonicated to remove adsorbed particles. Posteriorly the electrodes were cycled (20 scans) in PBS using CV at a scan rate of 100  $\text{mV s}^{-1}$  in a potential window of 0–1.0 V. Finally, 12 drops of 2.50  $\mu\text{L}$  of the dispersion of the nanotubes were deposited upon the electrode's surface. The electrodes were dried at room temperature after each drop deposition and were cycled (CV, 20 scans) in PBS at a scan rate of 100  $\text{mV s}^{-1}$  in a potential window of 0–1.0 V.

Morphological and surface characterization of GCE, GCE/OMWCNT-N without and submerged in a 2.50 g  $\text{L}^{-1}$  yeast concentration were performed by scanning electron microscopy (SEM) (thermionic) JEOL-JSM 6490LV equipped with a secondary electron detector (SEI) and backscatter (BES) using different augments. For the electrochemical characterization of the electrodes, cyclic voltammograms were recorded in potassium ferricyanide ( $\text{K}_3[\text{Fe}(\text{CN})_6]$ )  $1 \times 10^{-3}$  mol  $\text{L}^{-1}$  in 0.10 mol  $\text{L}^{-1}$  KCl, at different scan rates (5, 20, 40, 80, 100, and 200  $\text{mV s}^{-1}$ ), and both, the electroactive area and the heterogeneous transfer constant were calculated.

### 2.3. Electrochemical measurements and determination of yeast

The pH effect on the anodic potential and current density (current/

electroactive area) of *S. cerevisiae* sp yeast was studied throughout an unifactorial experimental design, taking as a factor the pH with six levels (pH: 4.30, 4.94, 6.14, 7.08, 8.13, and 10.2). The peak potential and the anodic current were the response variables. The experimental unit was the dispersion of *S. cerevisiae* sp in PBS at a concentration of  $5.56 \text{ g L}^{-1}$ . The studies were carried out by CV, in a potential window of 0.0 V–1.0 V and a scan rate of  $100 \text{ mV s}^{-1}$ . The studies of scan rate effect had the same conditions except the scan rates used.

The yeast concentration effect was observed by different electroanalytical techniques. The studies by CV were carried out at a potential window of 0–1 volt (V), a scan rate of  $100 \text{ mV s}^{-1}$ . The measurements by square wave voltammetry (SWV) were in a range of 0.4–0.8 V, deposition time of 120 s, amplitude 70 mV, step 10 mV, and frequency of 50 Hz. Differential pulse voltammetry (DPV) measurements were in a potential window of 0–1 V, deposition time of 20 s, the amplitude of 20 mV. Chronoamperometry studies were at a potential of 0.85 V for 1200

s. Initially, the electrochemical cell contained PBS pH 7.00, and successive additions of 50  $\mu\text{L}$  of the  $50 \text{ g L}^{-1}$  yeast stock were made every 120 s.

The detection and quantification limits respectively were calculated as  $\text{LD} = (3 * \text{SD Blank})/m$  and  $\text{LQ} = (10 * \text{SD Blank})/m$  according to the methodology proposed by D. C. Harris (2007), where SD is the standard deviation of the blank, and m the slope of the calibration curve. Statistical analyses were performed using Statgraphics® Centurion XVI.

### 3. Results and discussion

#### 3.1. Characterization of modified electrodes

Fig. 1A and Fig. 1D show SEM micrographs of glassy carbon electrode surface without modifying and modified with OMWCNT-N, respectively. Fig. 1D shows clusters of nanotubes that are distributed

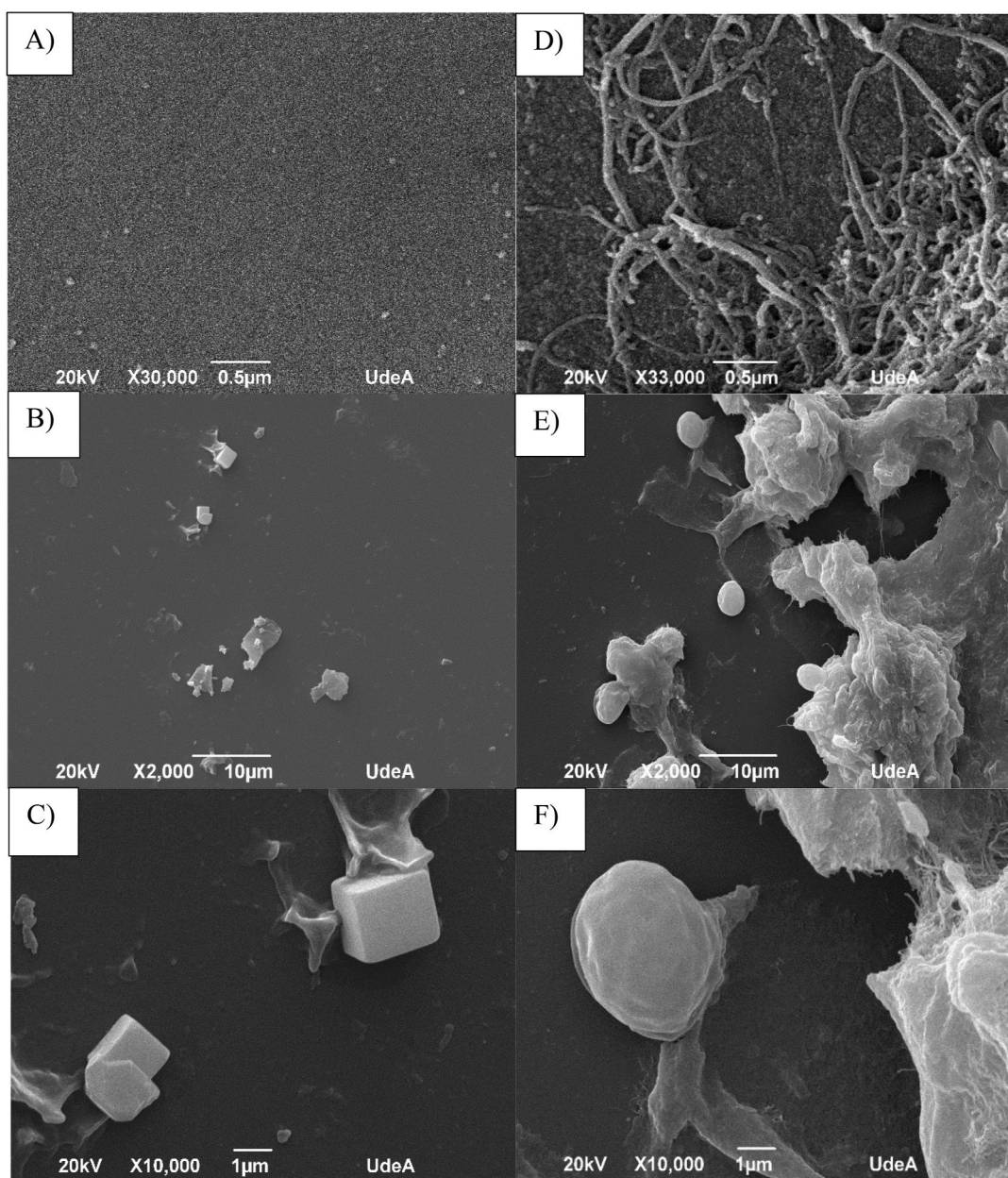


**Fig. 1.** SEM micrographs of (A) GCE before submerging in  $2.5 \text{ g L}^{-1}$  yeast suspension (B) and (C) GCE after submerging in  $2.5 \text{ g L}^{-1}$  yeast suspension at 2000x and 10000 respectively. (D) GCE/OMWCNT-N before submerging in  $2.5 \text{ g L}^{-1}$  yeast suspension (E) and (F) GCE/OMWCNT-N after submerging in  $2.5 \text{ g L}^{-1}$  yeast suspension at 2000x and 10000 respectively.

on the surface of the electrode, and the typical structure of the nanotubes can be observed.

Micrographs of GCE (Fig. 1B and C) after submerged in a  $2.50 \text{ g L}^{-1}$  yeast suspension show that the microorganism does not adhere to the glassy carbon surface. Attached to the surface, only can be observed the potassium chloride crystals, reactive used as supporting electrolyte.

Micrographs of the GCE/OMWCNT-N after submerged in the  $2.50 \text{ g L}^{-1}$  yeast suspension show sites without covering, and others covered with carbon nanotubes in which *Saccharomyces cerevisiae* sp cells are attached (Fig. 1E). An augment of the image (Fig. 1F) shows that the microorganism cells are attached to the carbon nanotubes instead of the glassy carbon surface. This phenomenon was present across the entire surface of the sensor. It indicates that the yeast has a higher affinity to the nanomaterial, and it has sense if we consider the low capability of absorption of the glassy carbon (Sharma, 2018).

Fig. 2 shows the cyclic voltammetry studies conducted in the  $\text{K}_3[\text{Fe}(\text{CN})_6] \cdot 3\text{H}_2\text{O}$  solution as a redox reference system.

Fig. 2A and B shows that the presence of OMWCNT-N increases both the anodic and cathodic current peaks and that the difference between the oxidation and reduction of potential decreases, indicating a higher electron transfer rate. According to Cheng et al. (2008), these facts are related to the presence of the nanotubes, which increase the number of active sites on which the accumulation of the electroactive compound can occur, also increasing the heterogeneous transfer constant.

Fig. 2C shows the expected typical behavior of a diffusion-controlled system according to the Randles – Sevcik equation, with a linear relationship between the current and the square root of the scan rate. The electroactive area was determined using the slope of the graph of the peak current vs. the square root of the scan rate, considering the number of electrons ( $n$ ) is equal to 1, the  $(\text{K}_3[\text{Fe}(\text{CN})_6])$  concentration  $1 \times 10^{-3} \text{ mol L}^{-1}$ , and the diffusion coefficient ( $D$ )  $7.60 \times 10^{-6} \text{ cm}^2 \text{ s}^{-1}$ . The

presence of the nanotubes increases the area up to 120.7% compared to the GCE unmodified. The reported results of Table 1 are adjusted to a normal distribution according to the Shapiro – Wilk test ( $p = 0.14$ ). The Grubbs test shows that there are no atypical values at a 95% confidence level, indicating good reproducibility of the electroactive areas of the modified electrodes.

With the difference between the anodic and cathodic potentials obtained in the CV experiments, we calculated the heterogeneous transfer constant ( $^0k$ ), considering  $\alpha = 0.5$  (assuming that the ratio between the anodic and cathodic peak currents  $i_{pa}/i_{pc}$  is close to 1) according to the methodology proposed by Nicholson (1965). The heterogeneous transfer constant increased by 24.8% in the GCE/OMWCNT-N.

The increases in both the electroactive area and the heterogeneous transfer constant can be attributed to the characteristics of OMWCNT. The nanotubes improve the availability of active zones where the reaction can occur, and the charge transfer process will be accomplished (Kumar and Vicente-Beckett, 2012). Nafion® is also a conductive ion exchange membrane, chemically inert, with excellent thermal stability, biocompatible, which also favors charge transport and its polar side chains facilitate the enveloping and dispersion of nanotubes (Guo et al., 2011; Lian et al., 2011; Peng et al., 2017; Wang et al., 2003).

**Table 1**  
GCE and GCE/OMWCNT-N electrode parameters.

Electrode	EA ( $\text{mm}^2$ )	$k$ ( $\times 10^{-3} \text{ cm s}^{-1}$ )
GCE	$8.20 \pm 0.40$	$2.26 \pm 0.92$
GCE/OMWCNT-N	$18.1 \pm 1.00$	$2.82 \pm 0.01$

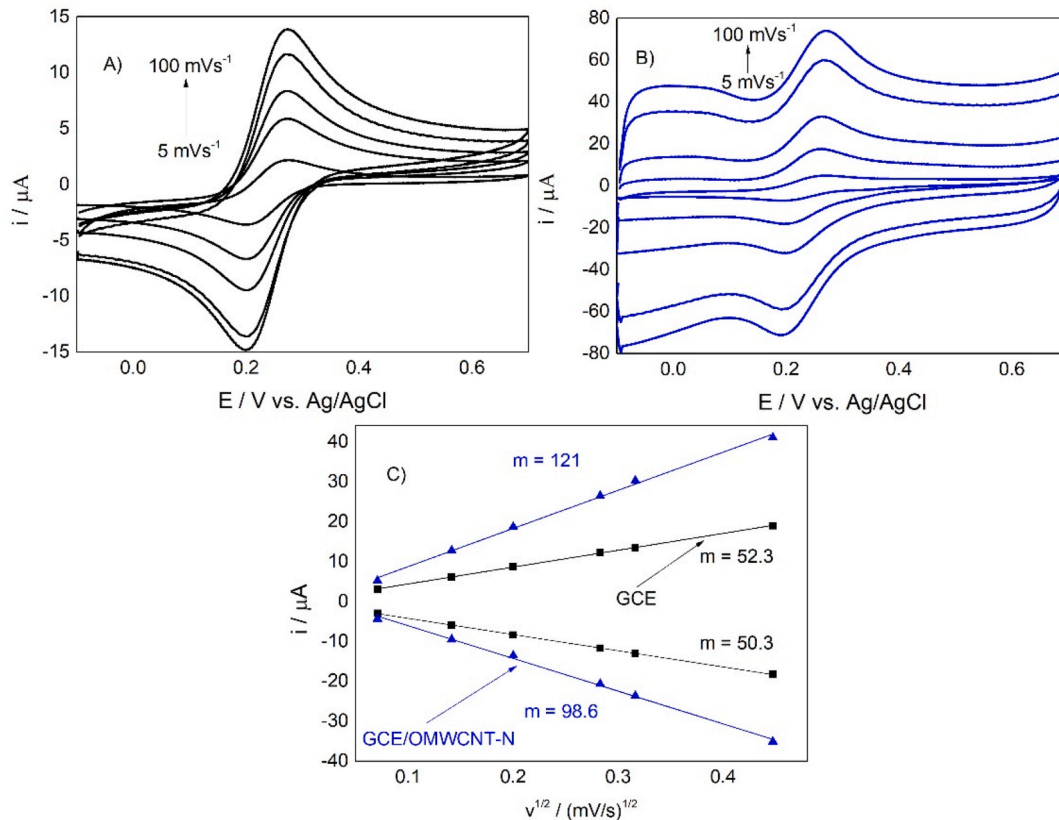


**Fig. 2.** Comparison of CVs for the (A) GCE and (B) GCE/OMWCNT-N. (C) Graph of current vs. the square root of the scan rate ( $i$  vs  $v^{1/2}$ ) for GCE (black rectangle) and GCE/OMWCNT-N (blue triangle). Cyclic voltammograms were obtained at different scan rates starting from 5, 20, 40, 80, and  $100 \text{ mV s}^{-1}$ . (For interpretation of the references to colour in this figure legend, the reader is referred to the Web version of this article.)

### 3.2. Electrochemical response of *Saccharomyces cerevisiae* on GCE/OMWCNT-N

#### 3.2.1. Effect of pH

Fig. 3 shows the effect of pH on anodic potential and current density. Fig. 3A shows the incidence of pH on the peak potential. There is no reaction at pH values less than 3.01 (data not shown), but as the pH increases, the electrochemical reaction starts, and the peak potential decreases. This result agrees with Matsunaga and Namba (1984), in which a similar study was conducted but using an electrochemical mediator. The relationship between the peak potential and pH shows a linear trend with a Pearson correlation coefficient  $r$  of  $-0.98$ . Also, ANOVA analysis shows that the factor “pH” has a significant influence on the peak potential ( $p = 0.00$ ). The results adjusted to a normal distribution, according to the Shapiro – Wilk test ( $p = 0.16$ ). The slope of the equation (0.029) that relates the potential and pH suggests the intervention of protons (Gonçalves et al., 2021) and two electrons in the electrode processes (Gowda and Nandibewoor, 2013).

Fig. 3B shows the behavior of the current density as a function of the pH. The figure shows that the current density increases at pH between 4.30 and 7.08 and decreases when the pH is above 7.08. However, according to an ANOVA analysis, pH has no significant influence on the current density ( $p = 0.66$ ). The results adjusted to a normal distribution, according to the Shapiro – Wilk test ( $p = 0.15$ ). The highest current density was at pH 7.08 then this value was chosen as the working pH for the studies of scan rates and concentration yeast effects.

The pH of the medium affects the gradient around the yeast’s cell membrane, the ATPase activity, and the intracellular pH influencing energy generation and cellular growth (Carmelo et al., 1996; Orij et al., 2009). Orij et al. (2009) did find that external pH values between 7.00 and 7.20 do not affect the internal pH, but that an external pH higher than the internal (7.20) increases the latter, decreasing cell growth. Therefore, there is an affection for cellular metabolism. These facts explain the decline in the current density observed in Fig. 3B.

#### 3.2.2. Effect of scan rate

The nanotubes modification effect was performed at  $2.50 \text{ g L}^{-1}$  of yeast suspensions at  $100 \text{ mV s}^{-1}$  on GCE/OMWCNT-N and GCE without modification. The voltammetric studies on  $5.00 \text{ g L}^{-1}$  yeast suspensions served to analyze the scan rate effect. All measurements used a potential window between 0.0 V and 1.0 V and pH 7.00. The peak potential (E) vs. logarithm of the scan rate plot served to evaluate the irreversibility of the process. Graphs of current density vs. square root of the scan rate and vs. scan rate allowed verifying if the process was diffusion- or adsorption-controlled. Through the Laviron methodology, the number

of electrons involved in the reaction was calculated (Laviron, 1979).

Fig. 4 shows the voltammetric behavior of *Saccharomyces cerevisiae* sp on GCE, GCE/OMWCNT-N, and at different scan rates.

Fig. 4A shows an acute anodic peak, located approximately at 0.70 V, absent on GCE without modification, which is related to the high affinity of the microorganism for the nanotubes instead of the glassy carbon surface, a fact evidenced in the SEM images, and indicate that the yeast joins to the electrode through the nanotubes. The nanotubes facilitate direct electron transfer (Saifuddin et al., 2013), and it explains why, without nanotubes, the electrochemical response of yeast is not observable. The process is irreversible since a peak in the cathodic sense was not observed in the potential window studied. This last fact agrees with Matsunaga & Namba’s (Matsunaga and Namba, 1984) study.

Fig. 4B indicates a dependence of the current intensity and the peak potential with the scan rate. When the scan rate increases, the current intensity increases, and the potential moves toward more positive values. This phenomenon is common in quasi-reversible and irreversible processes whose kinetics reaction is slow, and the equilibria are not reached rapidly, compared to the voltage of the scan rate. So the current takes more time to respond to the applied voltage, and the potential of the maximum current depends on the scan rate (Sandford et al., 2019). Further, Hulbert and Shain (Hulbert and Shain, 1970) explained that the dependence of the potential with the scan rate is due to the quick arrival of electroactive species to the electrode surface. It causes repulsion between them, and the number of electroactive species increases, requiring more energy for its reaction. Fig. 4C shows a linear relationship between the peak potential and the logarithm of the scan rate ( $R^2 = 96.5$ ). That behavior corresponds to an electrochemical reaction of the EC type (electrochemical reaction followed by an irreversible chemical reaction) (Chandra et al., 2008; Gowda and Nandibewoor, 2013). This behavior is similar to the adenine amino acid present in the structure of the CoA on multi-walled carbon nanotubes – ionic liquid composite film modified carbon paste electrode presented by Arvand et al. (2012). The yeast behavior is also similar to the electrochemical response of tryptophan amino acid. Ufnalska et al. (2020) proposed that the electrochemical signal of yeast is due to tryptophan residues presented in peptides involved in yeast reproduction. Other authors also showed the relationship between cell growth in fermentation processes and tryptophan (Álvarez-Fernández et al., 2019; Dei Cas et al., 2021; Fernández-Cruz et al., 2017).

As the process is irreversible, the  $E_p$  can be expressed according to Laviron’s expression (1), from which the product between the electronic transfer coefficient ( $\alpha$ ) and the number of electrons participating in the process ( $n$ ) can be calculated (Buddanavar and Nandibewoor, 2015).

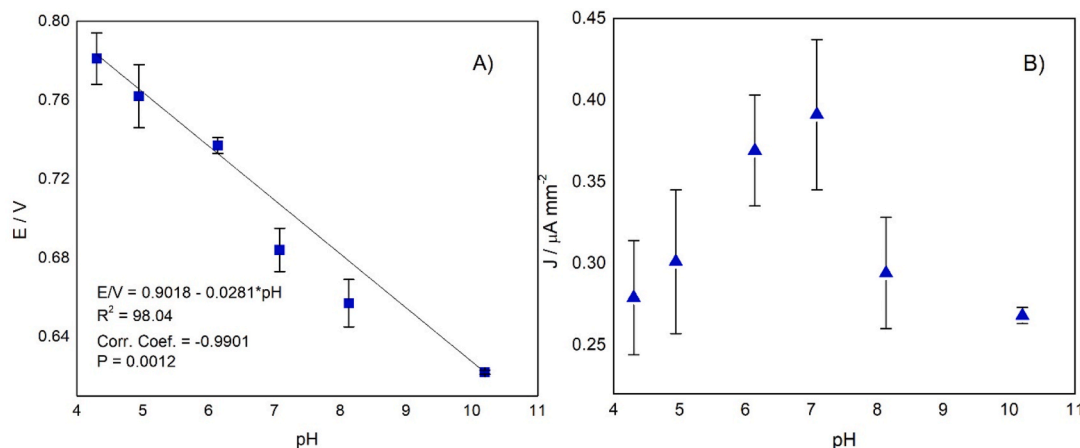


Fig. 3. The effect of pH on (A) the anodic potential (B) on the current density of *S. cerevisiae* sp. All measurements were made in PBS  $0.01 \text{ mol L}^{-1}$  with KCl  $0.1 \text{ mol L}^{-1}$ , at a scan rate of  $100 \text{ mV s}^{-1}$ .

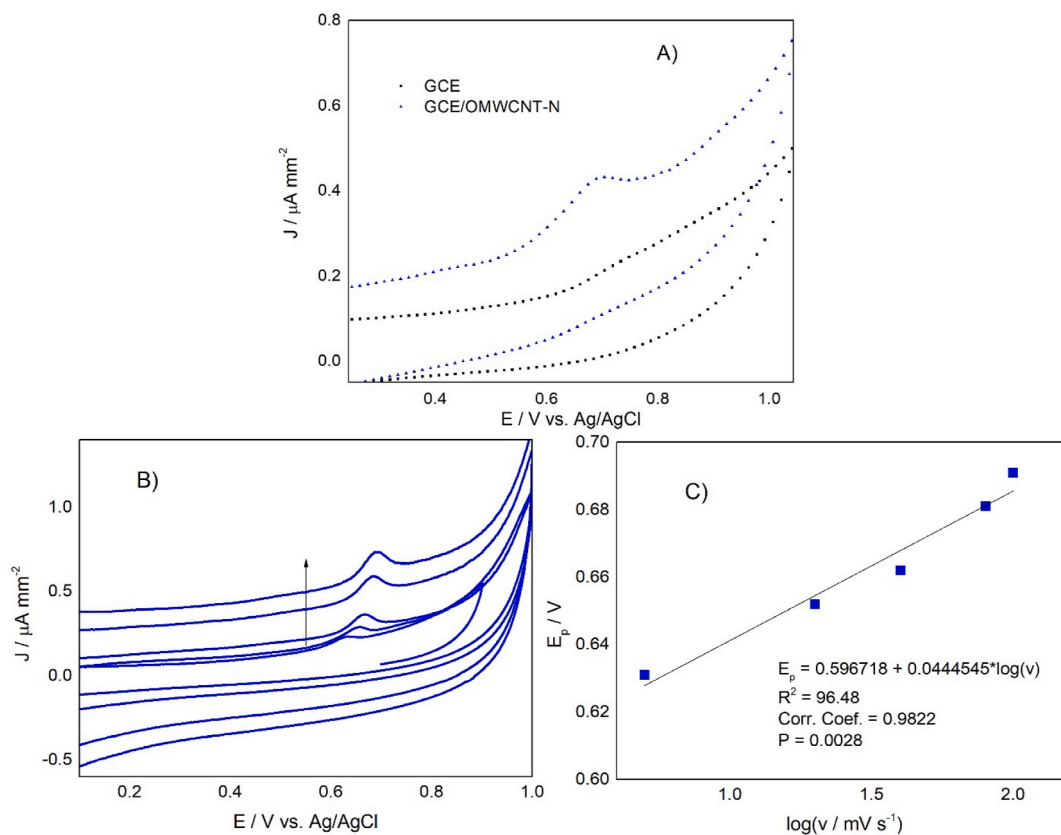


Fig. 4. (A) Electrochemical response of yeast on GCE (black rectangle) and GCE/OMWCNT-N (blue triangle) at  $100 \text{ mV s}^{-1}$  (B) Effect of the scan rate on the yeast anodic current at 5.0, 20, 40, 80, and  $100 \text{ mV s}^{-1}$ . (C) Anodic potential versus the logarithm of the scan rate. (For interpretation of the references to colour in this figure legend, the reader is referred to the Web version of this article.)

$$E_p = E^0 + \left(\frac{2.303RT}{\alpha nF}\right) \cdot \log\left(\frac{RTk^0}{\alpha nF}\right) + \left(\frac{2.303RT}{\alpha nF}\right) \cdot \log(v) \quad (1)$$

where  $\alpha$  is the electronic transfer coefficient,  $k^0$  the heterogeneous transfer constant of the reaction,  $n$  is the number of electrons transferred,  $v$  the scan rate,  $E^0$  is the formal redox potential,  $T = 298 \text{ K}$ ,  $R = 8.314 \text{ J K}^{-1} \text{ mol}^{-1}$ , and  $F = 96480 \text{ C mol}^{-1}$ . Using these values in the expression  $E_p = (2.303RT/\alpha nF) \cdot \log(v)$ , and considering the slope of Fig. 4C, the product  $\alpha n$  was 1.33.

Alternatively, according to Laviron (Laviron, 1974, 1979), equation (2) expressed the peak width in an irreversible process.

$$P_{width} = \left(\frac{62.5}{(1-\alpha)n}\right) [mV] \quad (2)$$

From equation (2), and using a peak width of 105 mV obtained from the cyclic voltammogram at a scan rate of  $100 \text{ mV s}^{-1}$ , we obtain that  $\alpha n = n - 0.625 \text{ mV}$ . Replacing the value for  $\alpha n = 1.33$  determined previously, we found that  $n = 1.93 \approx 2$  electrons. The same calculation was

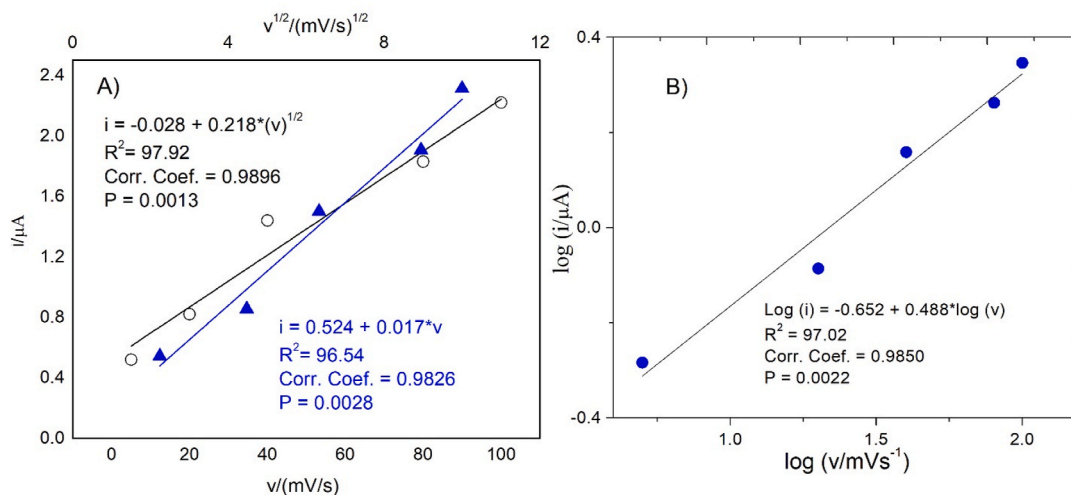


Fig. 5. (A) Effect of the square root of the scan rate (white circles) and scan rate (blue triangles) in the anodic current of yeast *S. cerevisiae* sp. (B)  $\log(i)$  vs.  $\log(v)$ . (For interpretation of the references to colour in this figure legend, the reader is referred to the Web version of this article.)

made for different scan rates in the range of  $5.0 \text{ mV s}^{-1}$  to  $100 \text{ mV s}^{-1}$ , obtaining similar results (2.21, 2.21, 2.02, 2.04, and 1.93 electrons for 5, 20, 40, 80, and  $100 \text{ mV s}^{-1}$  respectively). This result agrees with the report by Han et al. (2000).

Fig. 5 shows a linear relationship between the current vs. scan rate, the square root of the scan rate in the range between  $5.0 \text{ mV s}^{-1}$  to  $100 \text{ mV s}^{-1}$ , and  $\log(i)$  vs.  $\log(v)$ .

The linearity exhibited by the relationship between the current vs. the square root of scan rate and the slope (0.489) of the graph  $\log(i)$  vs.  $\log(v)$  indicates a diffusional control. The graph current vs. the scan rate is also linear, so the electrochemical response of *S. cerevisiae* can also be modeled by an adsorption-governed process. For this type of behavior, when there is no significant difference between both types of control, the process has a mixed control (Geng et al., 2016; Goyal et al., 2006). Matsunaga and Namba (1984) reported the diffusive component but didn't mention adsorptive effects. In this study, SEM micrographs of Fig. 1E and F, in which we can see incrustated cells yeast in the matrix of nanotubes, corroborated the adsorptive component.

### 3.3. Effect of concentration in the anodic current of *Saccharomyces cerevisiae* by different electroanalytical techniques

Fig. 6 shows the calibration curves of current density vs yeast concentration obtained through different electroanalytical techniques, using GCE/OMWCNT-N as the working electrode. The inserts in Fig. 6 present the electrochemical responses.

Cyclic voltammetry (CV), square wave voltammetry (SWV), differential pulse voltammetry (DPV), and chronoamperometry analysis were made to identify the suitable electroanalytical technique for the

determination of *Saccharomyces cerevisiae* sp. Table 2 shows the found analytical parameters.

The curve obtained by CV (Fig. 6A) has high dispersion, high detection limit, the sensitivity is low, and there is no linear relationship ( $r \ll 0.95$ ), thus the technique is inappropriate for electrochemical quantification. It is logical since the CV is a technique used for physicochemical studies instead of analytical purposes. Although the curve obtained by SWV (Fig. 6B) exhibited linearity, it has a lower sensitivity and higher LOD and LOQ compared to other techniques. SWV is not recommended for irreversible reactions (Mirceski et al., 2018) what explains these facts. Fig. 6C corresponds to curves obtained by DPV presenting good sensitivity, LOD, and LOQ, but the linear relationship and the linear range are minor compared to the obtained by CA. CA (Fig. 6D) turned out the most suitable technique for the quantification of *S. cerevisiae* sp. The CA has higher reproducibility, higher linearity, acceptable analytical parameters, and the number of electrodes used is minor in relationship with the other techniques, a fact that reduces cost and analysis time.

**Table 2**  
Summary of analytical parameters.

Technique	Sensitivity/ ( $\mu\text{A} \cdot \text{L} / \text{g}^2 \cdot \text{mm}^2$ )	LOD/(g $\text{L}^{-1}$ )	LOQ/(g $\text{L}^{-1}$ )	R	Linear range/ (g $\text{L}^{-1}$ )
CV	0.05	1.82	6.06	0.90	6.06–9.00
SWV	0.02	2.03	6.75	0.97	6.75–15.0
DPV	0.12	0.15	0.49	0.95	0.49–2.50
CA	0.09	0.98	3.36	0.99	3.36–6.52

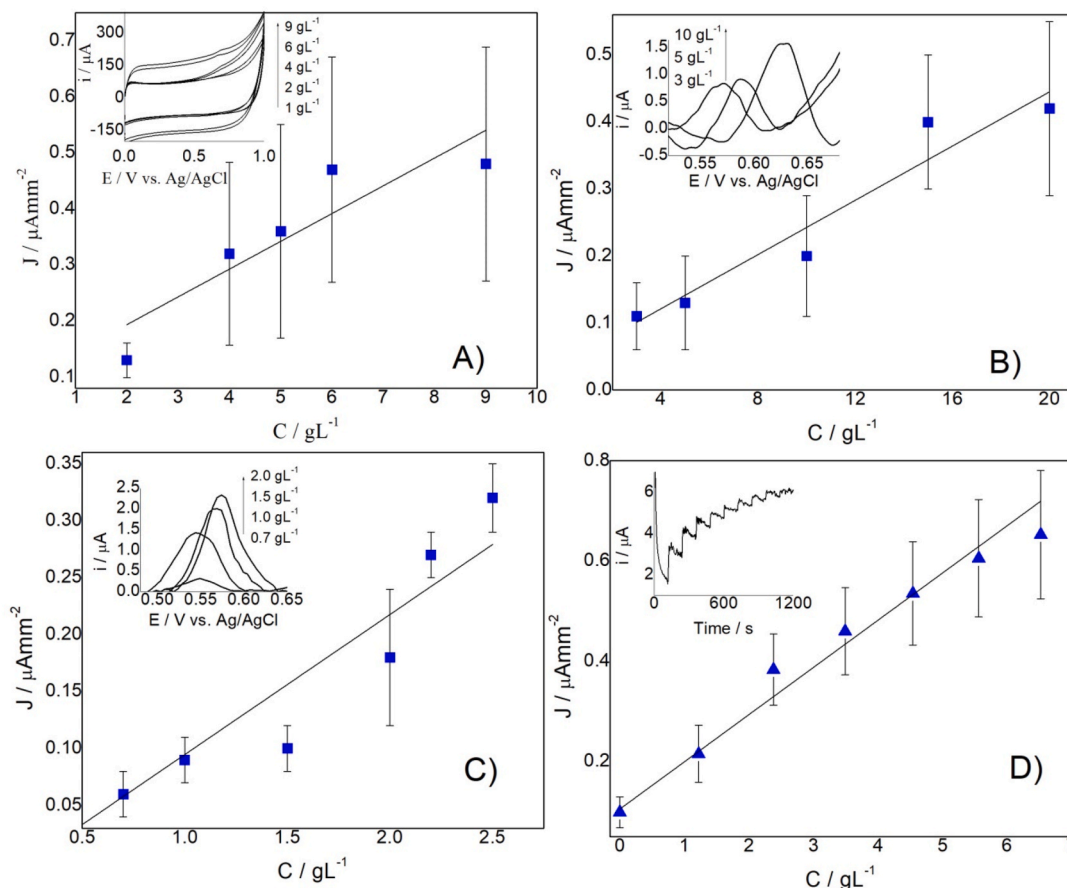


**Fig. 6.** Calibration curves for *Saccharomyces cerevisiae* sp using the GCE/OMWCNT-N and different electroanalytical techniques (A) CV, (B) SWV, (C) DPV, and (D) Chronoamperometry.

#### 4. Conclusions

Glassy carbon electrodes modified with OMWCNT-N dispersed in water and Nafion® promote the electrochemical oxidation of yeast *Saccharomyces cerevisiae* sp. The modification realized with the OMWCNT-N facilitates both the electroactive area and heterogeneous transfer constant increase. The studies showed that the electrochemical anodic potential of *Saccharomyces cerevisiae* sp depends on pH. Furthermore, the irreversibility of the process was confirmed and is consistent with an Electrochemical-Chemical (EC)-type mechanism and a mixed control of diffusion-adsorption, in which two electrons participate. This work allowed us to establish that the *Saccharomyces cerevisiae* sp determination can be carried out through chronoamperometry, getting acceptable analytical parameters, and using the fewer electrodes possible.

#### CRediT authorship contribution statement

**Isabel Acevedo Restrepo:** Methodology, Conceptualization, Validation, Formal analysis, Writing – original draft, Writing – review & editing, Funding acquisition. **Lucas Blandón Naranjo:** Methodology, Conceptualization, Formal analysis, Supervision, Funding acquisition. **Jorge Hoyos-Arbeláez:** Methodology, Formal analysis, Writing – review & editing. **Mario Víctor Vázquez:** Supervision, Project administration, Funding acquisition. **Silvia Gutiérrez Granado:** Methodology, Supervision. **Juliana Palacio:** Physical characterization.

#### Declaration of competing interest

The authors declare that they have no known competing financial interests or personal relationships that could have appeared to influence the work reported in this paper.

#### Acknowledgments

I.A.R would like to thank the Colombian entity for the Science, technology, and innovation – COLCIENCIAS (785–2017) for the doctoral scholarship and to the Electrochemistry group of the University of Guanajuato, México for the doctoral internship.

I.A.R, L.B.N, and M.V.V would like to thank the Committee for the Development of Research – CODI – of the University of Antioquia for the support of the project 2015–7523.

L.B.N would like to thank the post-doctoral stays program SNTel 2018 for its financial support.

J.H.A would like to thank the postdoctoral fellowship granted by Minciencias, convocatoria 848 de 2019.

#### References

- Akyilmaz, E., Erdoğan, A., Öztürk, R., Yaşa, I., 2007. Sensitive determination of l-lysine with a new amperometric microbial biosensor based on *Saccharomyces cerevisiae* yeast cells. *Biosens. Bioelectron.* 22 (6), 1055–1060. <https://doi.org/10.1016/j.bios.2006.04.023>.
- Álvarez-Fernández, M.A., Fernández-Cruz, E., García-Parrilla, M.C., Troncoso, A.M., Mattivi, F., Vrhovsek, U., Arapitsas, P., 2019. *Saccharomyces cerevisiae* and *Torulaspota delbrueckii* intra- and extra-cellular aromatic amino acids metabolism. *J. Agric. Food Chem.* 67 (28), 7942–7953. <https://doi.org/10.1021/acs.jafc.9b01844>.
- Arvand, M., Niazi, A., Mazhabi, R.M., Biparva, P., 2012. Direct electrochemistry of adenine on multiwalled carbon nanotube-ionic liquid composite film modified carbon paste electrode and its determination in DNA. *J. Mol. Liq.* 173, 1–7. <https://doi.org/10.1016/j.molliq.2012.06.004>. September 2012.
- Barlíková, A., Švorc, J., Miertuš, S., 1991. Hybrid biosensor for the determination of sucrose. *Anal. Chim. Acta* 247 (1), 83–87. [https://doi.org/10.1016/S0003-2670\(00\)83056-1](https://doi.org/10.1016/S0003-2670(00)83056-1).
- Blandón-Naranjo, L., Hoyos-Arbeláez, J., Vázquez, M.V., Della Pelle, F., Compagnone, D., 2018. NADH Oxidation onto different carbon-based sensors: effect of structure and surface-oxygenated groups. *J. Sensors* 2018. <https://doi.org/10.1155/2018/6525919>.

- Buddanavar, A.T., Nandibewoor, S.T., 2015. A simple and sensitive analytical tool for determination of ampyrone and its application in real sample analysis using carbon paste electrode. *Der Pharm. Lett.* 7 (12), 383–391.
- Campanella, L., Favero, G., Mostrofini, D., Tomassetti, M., 1996. Toxicity order of cholanic acids using an immobilised cell biosensor. *J. Pharmaceut. Biomed. Anal.* 14, 1007–1013. [https://doi.org/10.1016/0731-7085\(95\)01709-7](https://doi.org/10.1016/0731-7085(95)01709-7).
- Carmelo, V., Bogaerts, P., Sá-Correia, I., 1996. Activity of plasma membrane H<sup>+</sup>-ATPase and expression of PMA1 and PMA2 genes in *Saccharomyces cerevisiae* cells grown at optimal and low pH. *Arch. Microbiol.* 166 (5), 315–320. <https://doi.org/10.1007/s002030050389>.
- Chandra, U., Gilbert, O., Kumara Swamy, B.E., Bodke, Y.D., Sherigara, B.S., 2008. Electrochemical studies of eriochrome black t at carbon paste electrode and immobilized by sds surfactant: a cyclic voltammetric study. *Int. J. Electrochem. Sci.* 3 (9), 1044–1054.
- Cheng, Y., Liu, Y., Huang, J., Xian, Y., Zhang, W., Zhang, Z., Jin, L., 2008. Rapid amperometric detection of coliforms based on MWNTs/Nafion composite film modified glass carbon electrode. *Talanta* 75 (1), 167–171. <https://doi.org/10.1016/j.talanta.2007.10.047>.
- Ci, Y.-X., Feng, J., Jiang, Z.-w., Luo, D.-z., 1997. The voltammetric behavior of *Saccharomyces cerevisiae*. *Bioelectrochem. Bioenerg.* 43 (2), 293–296. [https://doi.org/10.1016/S0302-4598\(97\)00007-X](https://doi.org/10.1016/S0302-4598(97)00007-X).
- Corton, E., Raffa, D., Mikkelsen, S., 2001. A novel electrochemical method for the identification of microorganisms. *Electroanalysis* 13 (12), 999–1001. [https://doi.org/10.1002/1521-4109\(200108\)13:12<999::AID-ELAN999>3.0.CO;2-8](https://doi.org/10.1002/1521-4109(200108)13:12<999::AID-ELAN999>3.0.CO;2-8).
- Dei Cas, M., Vigentini, I., Vitalini, S., Laganaro, A., Iriti, M., Paroni, R., Foschino, R., 2021. Tryptophan derivatives by *saccharomyces cerevisiae* ec1118: evaluation, optimization, and production in a soybean-based medium. *Int. J. Mol. Sci.* 22 (1), 1–19. <https://doi.org/10.3390/ijms22010472>.
- Fernández-Cruz, E., Álvarez-Fernández, M.A., Valero, E., Troncoso, A.M., García-Parrilla, M.C., 2017. Melatonin and derived L-tryptophan metabolites produced during alcoholic fermentation by different wine yeast strains. *Food Chem.* 217, 431–437. <https://doi.org/10.1016/j.foodchem.2016.08.020>.
- Filipović, K., Mikšaj, Z., Šalamon, M., 2002. Cyanide determination in fruit brandies by an amperometric biosensor with immobilised *Saccharomyces cerevisiae*. *Eur. Food Res. Technol.* 215 (4), 347–352. <https://doi.org/10.1007/s00217-002-0564-4>. In this issue.
- Garjonyte, R., Melvydas, V., Malinauskas, A., 2006. Mediated amperometric biosensors for lactic acid based on carbon paste electrodes modified with baker's yeast *Saccharomyces cerevisiae*. *Bioelectrochem.* 68 (2), 191–196. <https://doi.org/10.1016/j.bioelechem.2005.08.002>.
- Geng, D., Li, M., Bo, X., Guo, L., 2016. Molybdenum nitride/nitrogen-doped multi-walled carbon nanotubes hybrid nanocomposites as novel electrochemical sensor for detection L-cysteine. *Sensor. Actuator. B Chem.* 237, 581–590. <https://doi.org/10.1016/j.snb.2016.06.127>.
- Gonçalves, A., Leoni, D., Diniz, L., 2021. A simple, fast, and direct electrochemical determination of tyramine in Brazilian wines using low-cost electrodes. *Food Control* 130, 108369. <https://doi.org/10.1016/j.foodcont.2021.108369>. June.
- Gowda, J.I., Nandibewoor, S.T., 2013. Electrochemical behavior of paclitaxel and its determination at glassy carbon electrode. *Asian J. Pharm. Sci.* 9 (1), 42–49. <https://doi.org/10.1016/j.ajps.2013.11.007>.
- Goyal, R.N., Gupta, V.K., Oyama, M., Bachheti, N., 2006. Differential pulse voltammetric determination of atenolol in pharmaceutical formulations and urine using nanogold modified indium tin oxide electrode. *Electrochem. Commun.* 8 (1), 65–70. <https://doi.org/10.1016/j.elecom.2005.10.011>.
- Guo, S., Wu, X., Zhou, J., Wang, J., Yang, B., Ye, B., 2011. MWNT/Nafion composite modified glassy carbon electrode as the voltammetric sensor for sensitive determination of 8-hydroxyquinoline in cosmetic. *J. Electroanal. Chem.* 655 (1), 45–49. <https://doi.org/10.1016/j.jelechem.2011.02.010>.
- Han, S., Li, X., Guo, G., Sun, Y., Yuan, Z., 2000. Voltammetric measurement of microorganism populations. *Anal. Chim. Acta* 405 (1–2), 115–121. [https://doi.org/10.1016/S0003-2670\(99\)00753-9](https://doi.org/10.1016/S0003-2670(99)00753-9).
- Harris, D.C., 2007. *Quantitative Chemical Analysis*, vol. 7. W.H. Freeman and Company. <https://doi.org/10.1016/B978-0-444-40826-6.50009-1>.
- Hartwell, L.H., 1974. *Saccharomyces cerevisiae* cell cycle. *Bacteriol. Rev.* 38 (2), 164–198. <https://doi.org/10.1128/membr.38.2.164-198.1974>.
- Hulbert, M.H., Shain, I., 1970. Rate-controlled adsorption of product in stationary electrode polarography. *Anal. Chem.* 42 (2), 162–171. <https://doi.org/10.1021/ac60284a020>.
- Kumar, S., Vicente-Beckett, V., 2012. Glassy carbon electrodes modified with multiwalled carbon nanotubes for the determination of ascorbic acid by square-wave voltammetry. *Beilstein J. Nanotechnol.* 3 (1), 388–396. <https://doi.org/10.3762/bjnano.3.45>.
- Laviron, E., 1974. Adsorption, autoinhibition and autocatalysis in polarography and in linear potential sweep voltammetry. *J. Electroanal. Chem.* 52 (3), 355–393. [https://doi.org/10.1016/S0022-0728\(74\)80448-1](https://doi.org/10.1016/S0022-0728(74)80448-1).
- Laviron, E., 1979. General expression of the linear potential sweep voltammogram in the case of diffusionless electrochemical systems. *J. Electroanal. Chem. Interfacial Electrochem.* 101, 19–28. [https://doi.org/10.1016/S0022-0728\(79\)80075-3](https://doi.org/10.1016/S0022-0728(79)80075-3).
- Legras, J.L., Merdinoglu, D., Cornuet, J.M., Karst, F., 2007. Bread, beer and wine: *Saccharomyces cerevisiae* diversity reflects human history. *Mol. Ecol.* 16 (10), 2091–2102. <https://doi.org/10.1111/j.1365-294X.2007.03266.x>.
- Lehmann, M.R., Riedel, K., Adler, K., Kunze, G., 2000. Amperometric measurement of copper ions with a deputy substrate using a novel *Saccharomyces cerevisiae* sensor. *Biosens. Bioelectron.* 15, 211–219. [https://doi.org/10.1016/S0956-5663\(00\)00060-9](https://doi.org/10.1016/S0956-5663(00)00060-9).



- Lian, H., Qian, W., Estevez, L., Liu, H., Liu, Y., Jiang, T., Wang, K., Guo, W., Giannelis, E. P., 2011. Enhanced actuation in functionalized carbon nanotube-Nafion composites. *Sensor. Actuator. B Chem.* 156 (1), 187–193. <https://doi.org/10.1016/j.snb.2011.04.012>.
- Matsunaga, T., Karube, I., Suzukis, 1979. Electrode system for the determination of microbial populations. *Appl. Environ. Microbiol.* 37 (1), 117–121. <https://doi.org/10.1128/AEM.37.1.117-121.1979>.
- Matsunaga, T., Namba, Y., 1984. Selective determination of microbial cells by graphite electrode modified with adsorbed 4,4-bipyridine. *Anal. Chim. Acta* 159, 87–94. [https://doi.org/10.1016/S0003-2670\(00\)84284-1](https://doi.org/10.1016/S0003-2670(00)84284-1).
- Mirceski, V., Skrzypek, S., Stojanov, L., 2018. Square-wave voltammetry. *ChemTexts* 4 (4). <https://doi.org/10.1007/s40828-018-0073-0>.
- Nicholson, R.S., 1965. *Analytical Chemistry*, vol. 37 issue 11 1965 [doi 10.1021\_ac60230a016].
- Orij, R., Postmus, J., Beek, A. Ter, Brul, S., Smits, G.J., 2009. In vivo measurement of cytosolic and mitochondrial pH using a pH-sensitive GFP derivative in *Saccharomyces cerevisiae* reveals a relation between intracellular pH and growth. *Microbiology* 155, 268–278. <https://doi.org/10.1099/mic.0.022038-0>.
- Peng, K.J., Lai, J.Y., Liu, Y.L., 2017. Preparation of poly(styrenesulfonic acid) grafted Nafion with a Nafion-initiated atom transfer radical polymerization for proton exchange membranes. *RSC Adv.* 7 (59), 37255–37260. <https://doi.org/10.1039/c7ra06984g>.
- Posseckardt, J., Schirmer, C., Kick, A., Rebatschek, K., Lamz, T., Mertig, M., 2018. Monitoring of *Saccharomyces cerevisiae* viability by non-Faradaic impedance spectroscopy using interdigitated screen-printed platinum electrodes. *Sensor. Actuator. B Chem.* 255, 3417–3424. <https://doi.org/10.1016/j.snb.2017.09.171>.
- Rawson, F., Gross, A., Garrett, D., Downard, A., Baronian, K., 2012. Mediated electrochemical detection of electron transfer from the outer surface of the cell wall of *Saccharomyces cerevisiae*. *Electrochem. Commun.* 15 (1), 5–87. <https://doi.org/10.1016/j.elecom.2011.11.030>.
- Saifuddin, N., Raziah, A.Z., Junizah, A.R., 2013. *Carbon Nanotubes : A Review on Structure and Their Interaction with Proteins*, 2013.
- Sandford, C., Edwards, M.A., Klunder, K.J., Hickey, D.P., Li, M., Barman, K., Sigman, M. S., White, H.S., Minter, S.D., 2019. A synthetic chemist's guide to electroanalytical tools for studying reaction mechanisms. *Chem. Sci.* 10 (26), 6404–6422. <https://doi.org/10.1039/c9sc01545k>.
- Sharma, S., 2018. *Glassy Carbon : A Promising Material for Micro-*. *Materials*, p. 11. <https://doi.org/10.3390/ma11101857>.
- Shen, T., Wu, Q., Xu, Y., 2021. Biodegradation of cyanide with *Saccharomyces cerevisiae* in Baijiu fermentation. *Food Control* 127, 108107. <https://doi.org/10.1016/j.foodcont.2021.108107>. January.
- Turker, M., 2014. Yeast biotechnology: diversity and applications. *Yeast Biotechnol.: Divers. Appl.* 1–26. <https://doi.org/10.1007/978-1-4020-8292-4>. December.
- Ufnalska, I., Wawrzyniak, U.E., Bossak-Ahmad, K., Bal, W., Wróblewski, W., 2020. Electrochemical studies of binary and ternary copper(II) complexes with  $\alpha$ -factor analogues. *J. Electroanal. Chem.* 862, 114003. <https://doi.org/10.1016/j.jelechem.2020.114003>.
- Valiūnienė, A., Petronienė, J., Dulkys, M., Ramanavičius, A., 2020. Investigation of Active and Inactivated Yeast Cells by Scanning Electrochemical Impedance Microscopy. *Electroanalysis* 32 (2), 367–374. <https://doi.org/10.1002/elan.201900414>.
- Villalonga, M., Borisova, B., Arenas, C., Villalonga, A., Arévalo, M., Sánchez, A., Pingarrón, J., Briones, A., Villalonga, R., 2019. Disposable electrochemical biosensors for *Brettanomyces bruxellensis* and total yeast content in wine based on core-shell magnetic nanoparticles. *Sensor. Actuator. B Chem.* 279, 15–21. <https://doi.org/10.1016/j.snb.2018.09.092>.
- Wang, J., Musameh, M., Lin, Y., 2003. Solubilization of carbon nanotubes by Nafion toward the preparation of amperometric biosensors. *J. Am. Chem. Soc.* 125 (9), 2408–2409. <https://doi.org/10.1021/ja028951v>.
- Zhao, J., Wang, Z., Fu, C., Wang, M., He, Q., 2008. The mediated electrochemical method for rapid fermentation ability assessment. *Electroanalysis* 20 (14), 1587–1592. <https://doi.org/10.1002/elan.200804218>.
- Zhong, L., Carere, J., Mats, L., Lu, Z., Lu, F., Zhou, T., 2021. Formation of glutathione patulin conjugates associated with yeast fermentation contributes to patulin reduction. *Food Control* 123, 107334. <https://doi.org/10.1016/j.foodcont.2020.107334>. May 2020.